Sullivan Process for Meson Structure

Wen-Chen Chang

January 8, 2025

Outline

- Sullivan process
  - In DIS process
  - In hadron-hadron interactions
- Meson PDFs studied by Sullivan process
  - In DIS process: a leading neutron in ep collisions
  - In hadron-hadron interactions: a leading neutron in proton-proton (pp) and proton-lead (pP b) collisions
- Summary

EIC: Sullivan Process

Meson Structure: Summary of EIC Detector Requirements

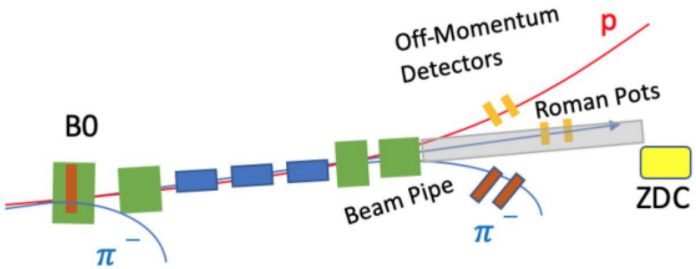

- **For π-n:**
  - Lower energies (5 on 41, 5 on 100) require at least 60 x 60 cm^2
  - For all energies, the neutron detection efficiency is 100% with the planned ZDC
- **For π-n and K^+/Λ:**
  - All energies need good ZDC angular resolution for the required -t resolution
  - High energies (10 on 100, 10 on 135, 18 on 275) require resolution of 1cm or better
- **K^+/Λ benefits from low energies (5 on 41, 5 on 100) and also need:**
  - $\Lambda \to n + \pi^0$: additional high-res/granularity EMCal+tracking before ZDC – seems doable
  - $\Lambda \to p + \pi^-$: additional trackers in opposite direction on path to ZDC – more challenging
- Standard electron detection requirements
- Good hadron calorimetry for good x resolution at large x

https://indico.bnl.gov/event/8315/contributions/36990/attachments/28487/43882/CFNS-Pion-Kaon-Structure-Horn-nbk.pdf
https://arxiv.org/abs/1907.08218 , https://arxiv.org/abs/2102.11788

Sullivan Process
[PRD 5, 1732 (1972)]

PHYSICAL REVIEW D VOLUME 5, NUMBER 7 1 APRIL 1972

One-Pion Exchange and Deep-Inelastic Electron-Nucleon Scattering

J. D. Sullivan*
National Accelerator Laboratory, Batavia, Illinois 60510
(Received 29 November 1971)

The role of one-pion exchange is examined in the deep-inelastic region for electron-nucleon scattering. Exclusive channels like πN, $\pi\Delta$ will contribute negligible, nonscaling contributions to σ_S. On the other hand, inclusive final states like N + "anything," where the detected final nucleon is slow in the lab system, afford the opportunity to experimentally determine the structure functions for electron-pion scattering provided the characteristic one-pion-exchange structure (dip or peak) is observed at small momentum transfer.

I. INTRODUCTION

Inelastic electron-proton experiments have been carried out recently in which hadrons are detected in coincidence with the scattered electron.[1] The region explored in these coincidence experiments does not yet overlap significantly with the region in which scaling has been established experimentally in inelastic electron-proton scattering.[2]

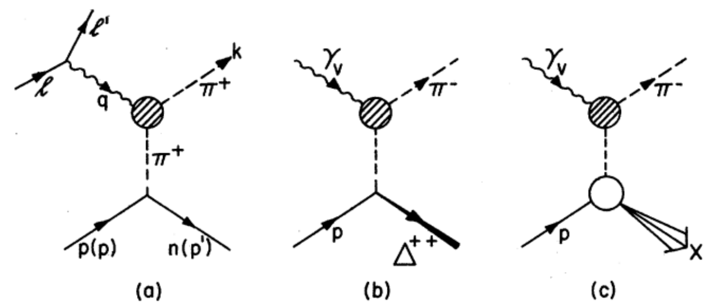

FIG. 1. (a) One-pion-exchange contribution to electroproduction of $\pi^+ n$. (b) Electroproduction of $\pi^-\Delta^{++}$ via π^- exchange. (c) Pion-current contributions to high-mass baryon states.

$\bar{d}/\bar{u}(x)$ from pp and pd Drell-Yan Process

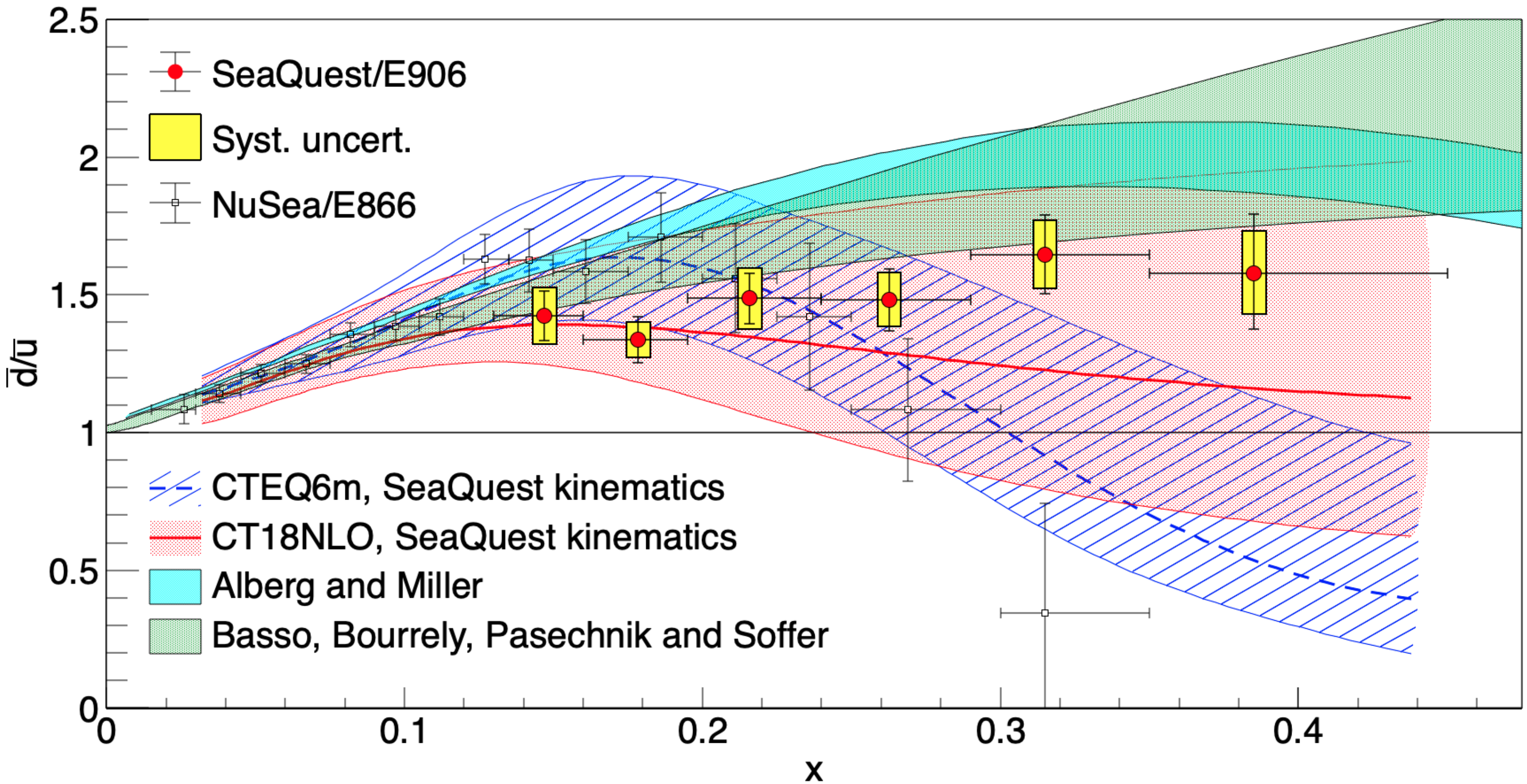

The extracted $\bar{\mathrm{d}}/\bar{u}(x)$ are consistent with CT18NLO and predictions of pion-cloud model.

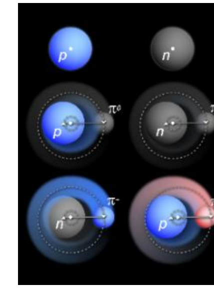

Origin of $\bar{u}(x) \neq \bar{d}(x)$: Non-perturbative QCD effect

- Meson cloud in the nucleons (Thomas 1983, Kumano 1991): Sullivan process in DIS.

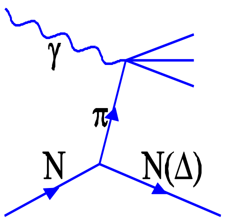

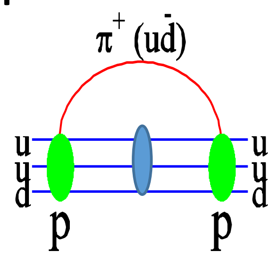

$$|p\rangle = \sqrt{Z}\,|p_0\rangle + a_{N\pi/p}\left[-\sqrt{\frac{1}{3}}|p_0\pi^0\rangle + \sqrt{\frac{2}{3}}|n_0\pi^+\rangle\right] + a_{\Delta\pi/p}\left[\sqrt{\frac{1}{2}}|\Delta_0^{++}\pi^-\rangle - \sqrt{\frac{1}{3}}|\Delta_0^{+}\pi^0\rangle + \sqrt{\frac{1}{6}}|\Delta_0^{0}\pi^+\rangle\right]$$

$$+ a_{\Lambda K/p}\,|\Lambda_0 K^+\rangle + a_{\Sigma K/p}\left[-\sqrt{\frac{1}{2}}|\Sigma_0^+K^0\rangle + \sqrt{\frac{1}{2}}|\Sigma_0^0 K^+\rangle\right] + \cdots$$

n

- Chiral quark model (Eichten et al. 1992; Wakamatsu 1992): Goldstone bosons couple to valence quarks.

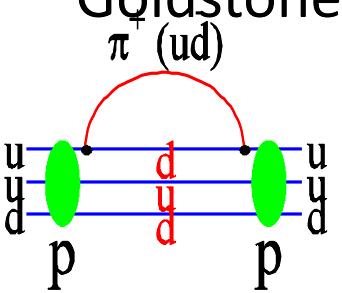

$$|U\rangle = \sqrt{Z}|u\rangle + \sqrt{\frac{1}{3}}a_{\pi/U}|u\pi^0\rangle + \sqrt{\frac{2}{3}}a_{\pi/U}|d\pi^+\rangle + a_{K/U}|sK^+\rangle + \cdots$$

$$|D\rangle = \sqrt{Z}|d\rangle + \sqrt{\frac{1}{3}}a_{\pi/D}|d\pi^0\rangle + \sqrt{\frac{2}{3}}a_{\pi/D}|u\pi^-\rangle + a_{K/D}|sK^0\rangle + \cdots,$$

Pion cloud is a source of antiquarks in the protons and it lead to $\bar{d} > \bar{u}$.

One-pion-exchange model

$$F_2^{\mathrm{LN}(3)}(x, Q^2, x_L) = 2 f_{\pi N}(\bar{x}_L) F_2^{\pi}(x_\pi, Q^2).$$

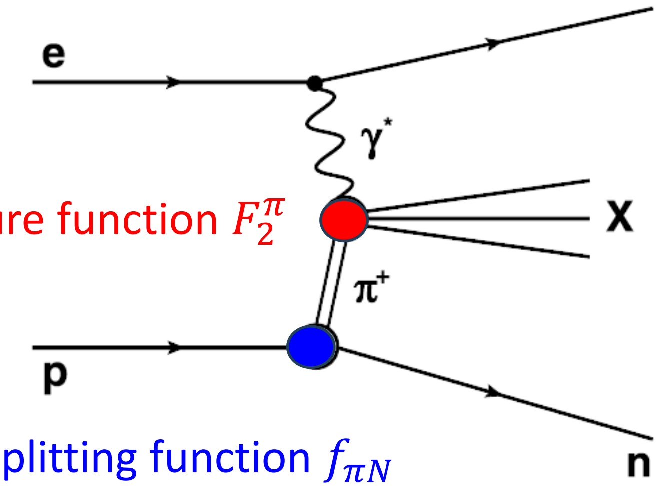

Pion structure function F_2^π

Splitting function $f_{\pi N}$

$$f_{\pi N}(\bar{x}_L) = \frac{g_A^2 M^2}{(4\pi f_\pi)^2} \int dk_\perp^2 \frac{\bar{x}_L [k_\perp^2 + \bar{x}_L^2 M^2]}{x_L^2 D_{\pi N}^2} |\mathcal{F}|^2,$$

$$\mathcal{F} = \begin{cases} \text{(i)} \ \exp((M^2 - s)/\Lambda^2) & s\text{-dep exponential} \\ \text{(ii)} \ \exp(D_{\pi N}/\Lambda^2) & t\text{-dep exponential} \\ \text{(iii)} \ (\Lambda^2 - m_\pi^2)/(\Lambda^2 - t) & t\text{-dep monopole} \\ \text{(iv)} \ \bar{x}_L^{-\alpha_\pi(t)} \exp(D_{\pi N}/\Lambda^2) & \text{Regge} \\ \text{(v)} \ [1 - D_{\pi N}^2/(\Lambda^2 - t)^2]^{1/2} & \text{Pauli-Villars} \end{cases}$$

Pion PDFs: JAM18
[Barry et al., PRL 121, 152001 (2018)]

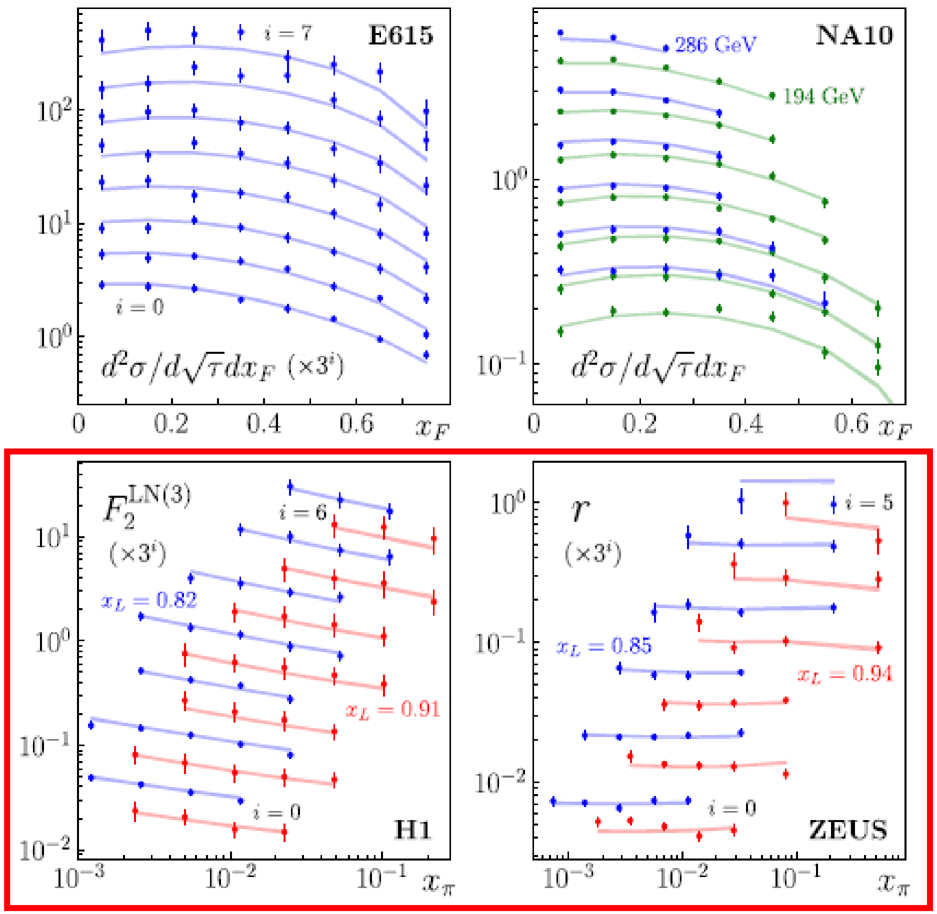

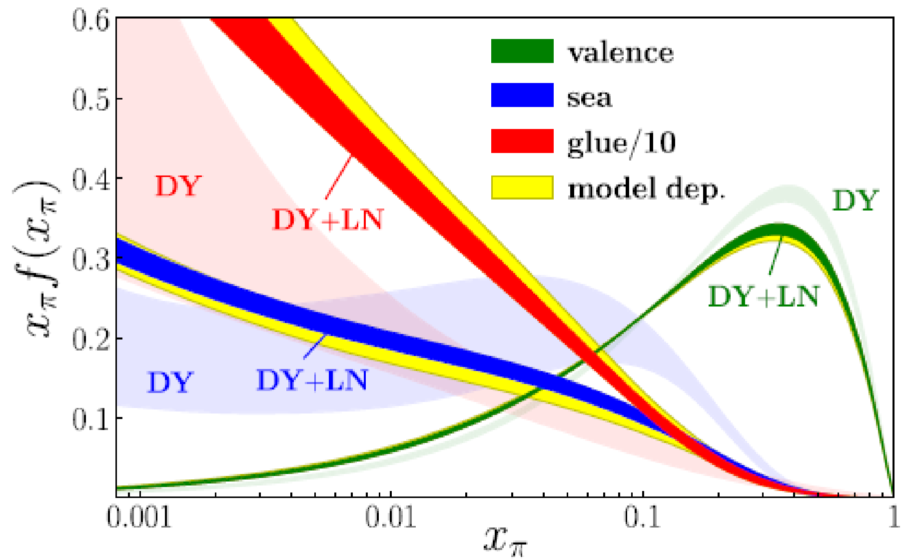

- Uncertainties are much reduced using DY+LN, as compared to DY alone.

Light Sea Quarks Asymmetry PRD 93, 054011 (2016)

$$|p\rangle = \sqrt{Z}\,|p_0\rangle + a_{N\pi/p}\left[-\sqrt{\frac{1}{3}}|p_0\pi^0\rangle + \sqrt{\frac{2}{3}}|n_0\pi^+\rangle\right] + a_{\Delta\pi/p}\left[\sqrt{\frac{1}{2}}|\Delta_0^{++}\pi^-\rangle - \sqrt{\frac{1}{3}}|\Delta_0^{+}\pi^0\rangle + \sqrt{\frac{1}{6}}|\Delta_0^{0}\pi^+\rangle\right]$$
$$+ a_{\Lambda K/p}\,|\Lambda_0 K^+\rangle + a_{\Sigma K/p}\left[-\sqrt{\frac{1}{2}}|\Sigma_0^+K^0\rangle + \sqrt{\frac{1}{2}}|\Sigma_0^0K^+\rangle\right] + \cdots$$

$$\bar{d} - \bar{u} = \left(f_{\pi^+ n} - \frac{2}{3} f_{\pi^-\Delta^{++}}\right) \otimes \bar{q}_v^{\pi}, \qquad (16)$$

where $\bar{q}_v^{\pi} \equiv \bar{d}^{\pi^+} - d^{\pi^+} = \bar{u}^{\pi^-} - u^{\pi^-}$ is the valence quark PDF in the pion and the symbol "$\otimes$" denotes the convolution integral $f \otimes q = \int_0^1 dy \int_0^1 dz f(y) q(z) \delta(x - yz)$.

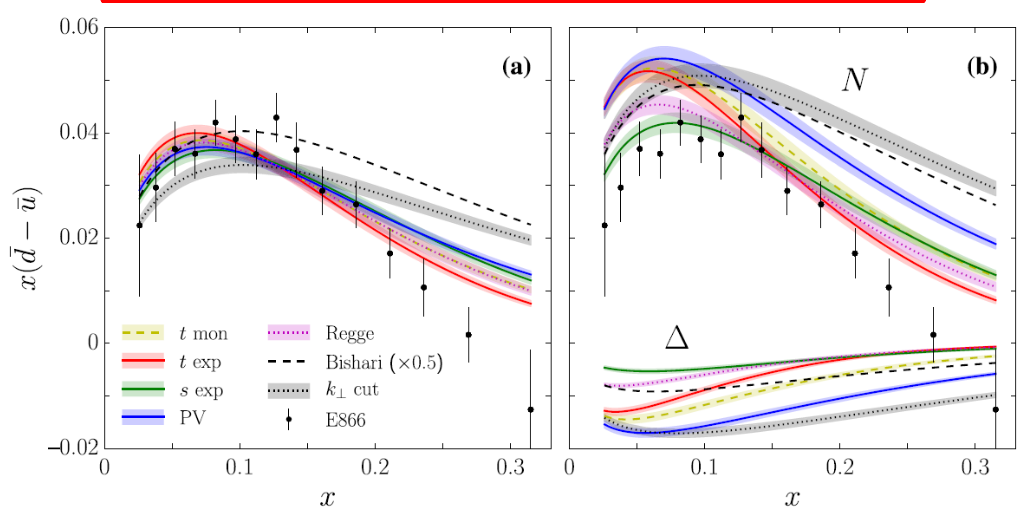

Past Measurements of Sullivan Process

- H1:
  - https://link.springer.com/article/10.1140/epjc/s10052-010-1369-4
  - https://arxiv.org/abs/1001.0532
- ZEUS:
  - https://www.sciencedirect.com/science/article/pii/S055032130200439X
  - https://arxiv.org/abs/hep-ex/0205076

Reaction Diagrams and Kinematic Variables Q^2, x, x_L, t

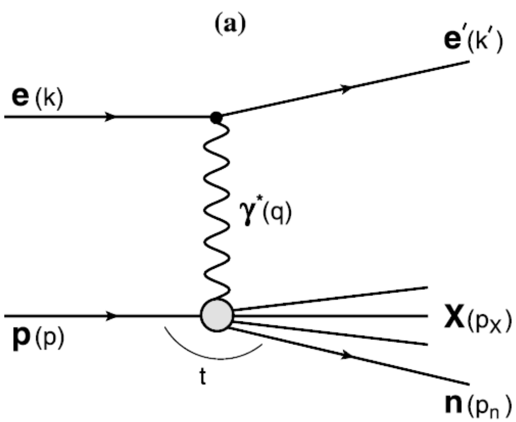

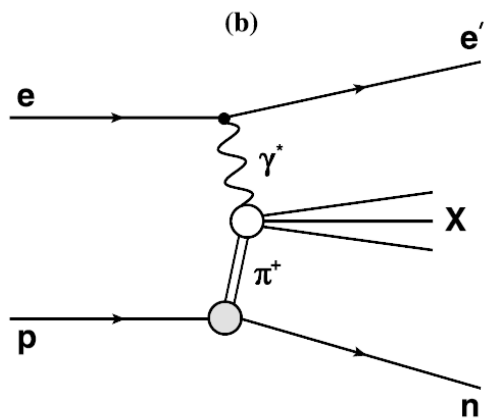

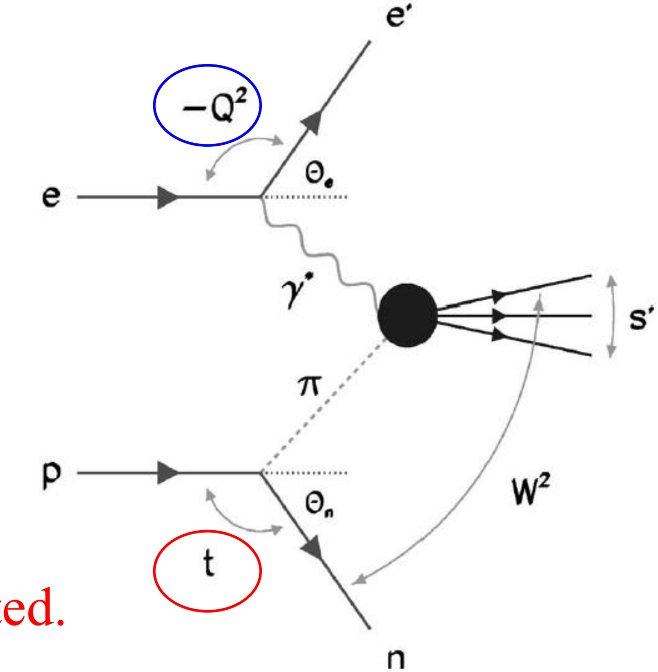

t and p_T of n are correlated.

$$Q^2 = -q^2, \qquad x = \frac{Q^2}{2p \cdot q}, \qquad y = \frac{p \cdot q}{p \cdot k},$$

$$y = q \cdot P/(k \cdot P) \simeq Q^2/(sx)$$

$$W^2 = (P + k - k')^2 = m_p^2 + Q^2(1 - x)/x$$

$$p_T \simeq x_L E_p \theta_n$$

$$x_L = 1 - \frac{q \cdot (p - p_n)}{q \cdot p} \simeq E_n/E_p,$$

$$t = (p - p_n)^2 \simeq -\frac{p_T^2}{x_L} - (1 - x_L)\left(\frac{m_n^2}{x_L} - m_p^2\right),$$

$$x_\pi = \frac{x}{1 - x_L}$$

forward neutron calorimeter (FNC)

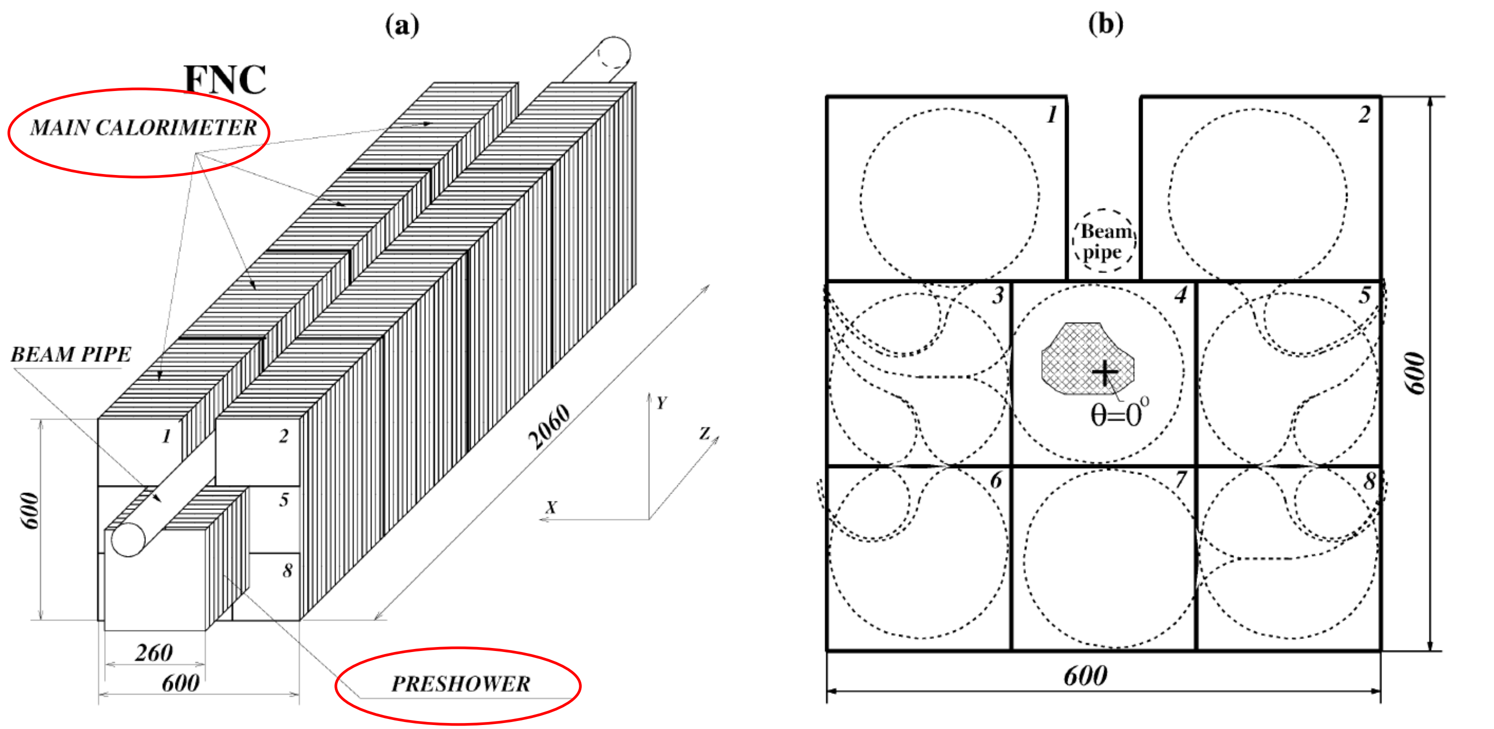

Fig. 2 (**a**) Schematic view of the FNC. (**b**) Layout of tiles on an active board of the Main Calorimeter; the position of readout fibres is indicated by *dotted lines*; the *hatched* area shows the geometrical acceptance window defined by the beam line elements. The position corresponding to $\theta = 0°$ is also indicated. All dimensions are given in mm

Event selection

The selection of DIS events is based on the identification of the scattered positron as the most energetic compact calorimetric deposit in the SpaCal with an energy $E'_e > 11$ GeV and a polar angle $156° < \theta'_e < 175°$. The energy weighted cluster radius is required to be less than 4 cm, as expected for an electromagnetic shower [32]. The z-coordinate of the primary event vertex is required to be within ±35 cm of the nominal position of the interaction point. The remaining clusters in the calorimeters and the charged tracks are combined to reconstruct the hadronic final state. To suppress events with initial state hard photon radiation, as well as events originating from non-ep interactions, the quantity $E - p_z$, summed over all reconstructed particles including the positron, is required to lie between 35 GeV and 70 GeV. This quantity is expected to be twice the electron beam energy for DIS events without QED radiation. Furthermore, events are selected within the kinematic range $6 < Q^2 < 100$ GeV^2, $0.02 < y < 0.6$ and $1.5 \cdot 10^{-4} < x < 3 \cdot 10^{-2}$.

Events containing a leading neutron are selected by requiring a hadronic cluster in the FNC with an energy above 275 GeV and a polar angle below 0.75 mrad. The cut on polar angle, defined by the geometrical acceptance of the FNC, restricts the neutron transverse momenta p_T to the range $p_T < x_L \cdot 0.69$ GeV.

Reaction Diagrams and Kinematic Variables Q^2, x, x_L, t

Leading-neutron cross section

$$\frac{d^4\sigma(ep \to enX)}{dx\, dQ^2\, dx_L\, dt} = \frac{4\pi\alpha^2}{x Q^4}\left(1 - y + \frac{y^2}{2}\right) F_2^{LN(4)}(Q^2, x, x_L, t).$$

Structure function

$$F_2^{\mathrm{LN}(3)}(x, Q^2, x_\mathrm{L}) \equiv \int_0^{p_\mathrm{T}^{\max}} F_2^{\mathrm{LN}(4)}(x, Q^2, x_\mathrm{L}, p_\mathrm{T})\, dp_\mathrm{T}$$

$$\frac{d^3\sigma(ep \to enX)}{dx\, dQ^2\, dx_L} = \int_{t_0}^{t_{\min}} \frac{d^4\sigma(ep \to enX)}{dx\, dQ^2\, dx_L\, dt}\, dt = \frac{4\pi\alpha^2}{x Q^4}\left(1 - y + \frac{y^2}{2}\right) F_2^{LN(3)}(Q^2, x, x_L),$$

where the integration limits are

$$t_{\min} = -(1 - x_L)\left(\frac{m_n^2}{x_L} - m_p^2\right) \quad \text{and}$$

$$t_0 = -\frac{(p_T^{\max})^2}{x_L} + t_{\min}.$$

H1

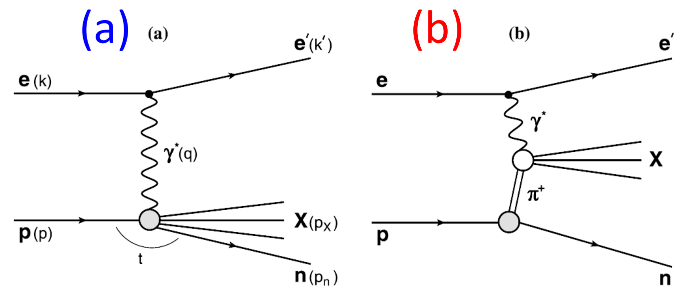

Eur. Phys. J. C (2010) 68: 381–399

Fig. 3 The observed neutron energy (**a**) and transverse momentum (**b**) distributions in the kinematic range $6 < Q^2 < 100\ \mathrm{GeV}^2$ and $1.5 \cdot 10^{-4} < x < 3 \cdot 10^{-2}$. The data are compared to the predictions of RAPGAP-π (*dashed line*) and DJANGO (*dotted line*) Monte Carlo simulations. Also shown is a weighted combination of those two simulations (*full line*), as described in Sect. 3.4

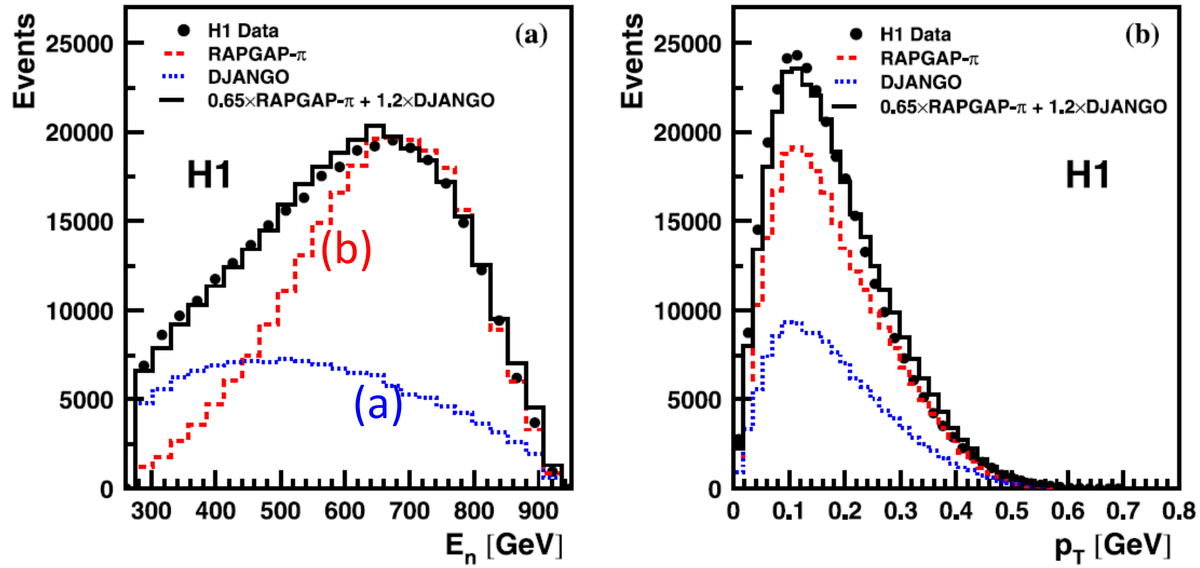

tion in this region. The best description of the data is achieved if the predictions of the RAPGAP-π and DJANGO Monte Carlo programs are added, using weighting factors of 0.65 and 1.2 for RAPGAP-π and DJANGO, respectively. This Monte Carlo combination is labelled as "0.65× RAPGAP-π + 1.2×DJANGO" in the figures and is used to correct the data.

H1

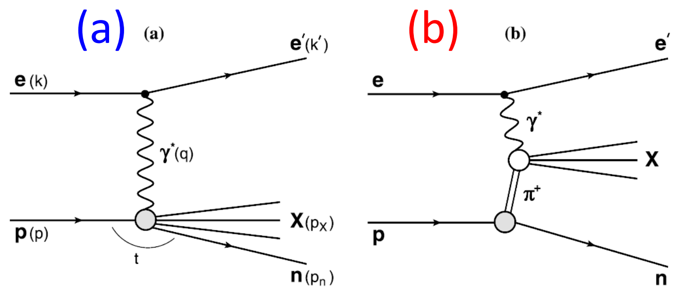
(a)
(b)
e (k)
e′(k′)
γ*(q)
p (p)
X(pX)
n (pn)
t
e
e′
γ*
π+
X
p
n

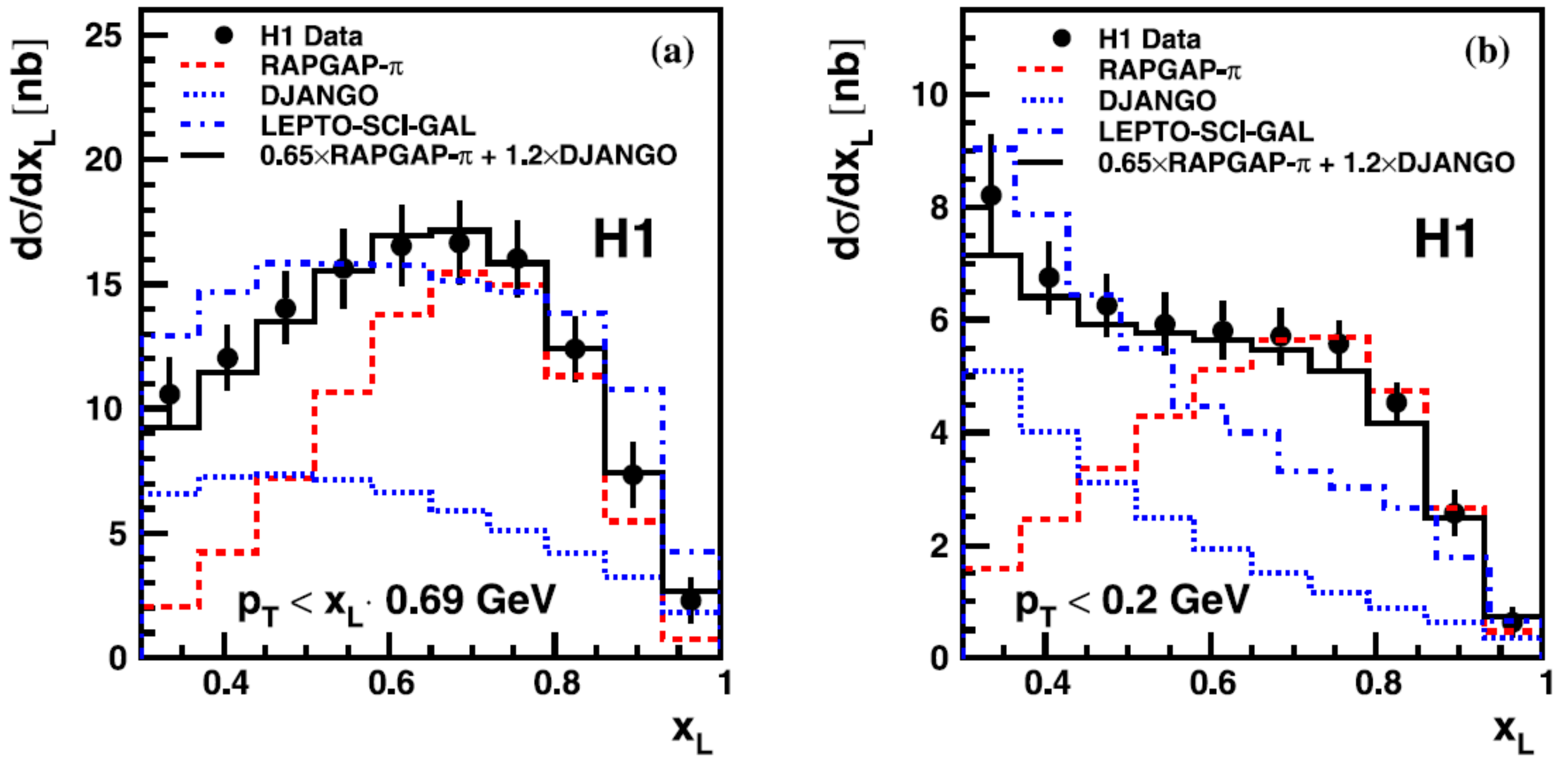
dσ/dxL [nb]
H1 Data
RAPGAP-π
DJANGO
LEPTO-SCI-GAL
0.65×RAPGAP-π + 1.2×DJANGO
(a)
(b)
H1
pT < xL · 0.69 GeV
pT < 0.2 GeV
xL

H1

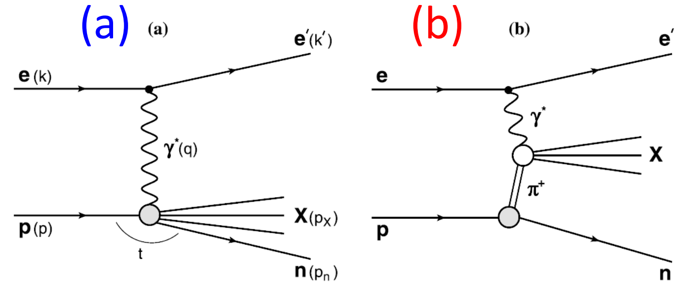
(a)
(a)
e (k)
e′(k′)
γ*(q)
p (p)
X (pX)
t
n (pn)
(b)
(b)
e
e′
γ*
X
π+
p
n

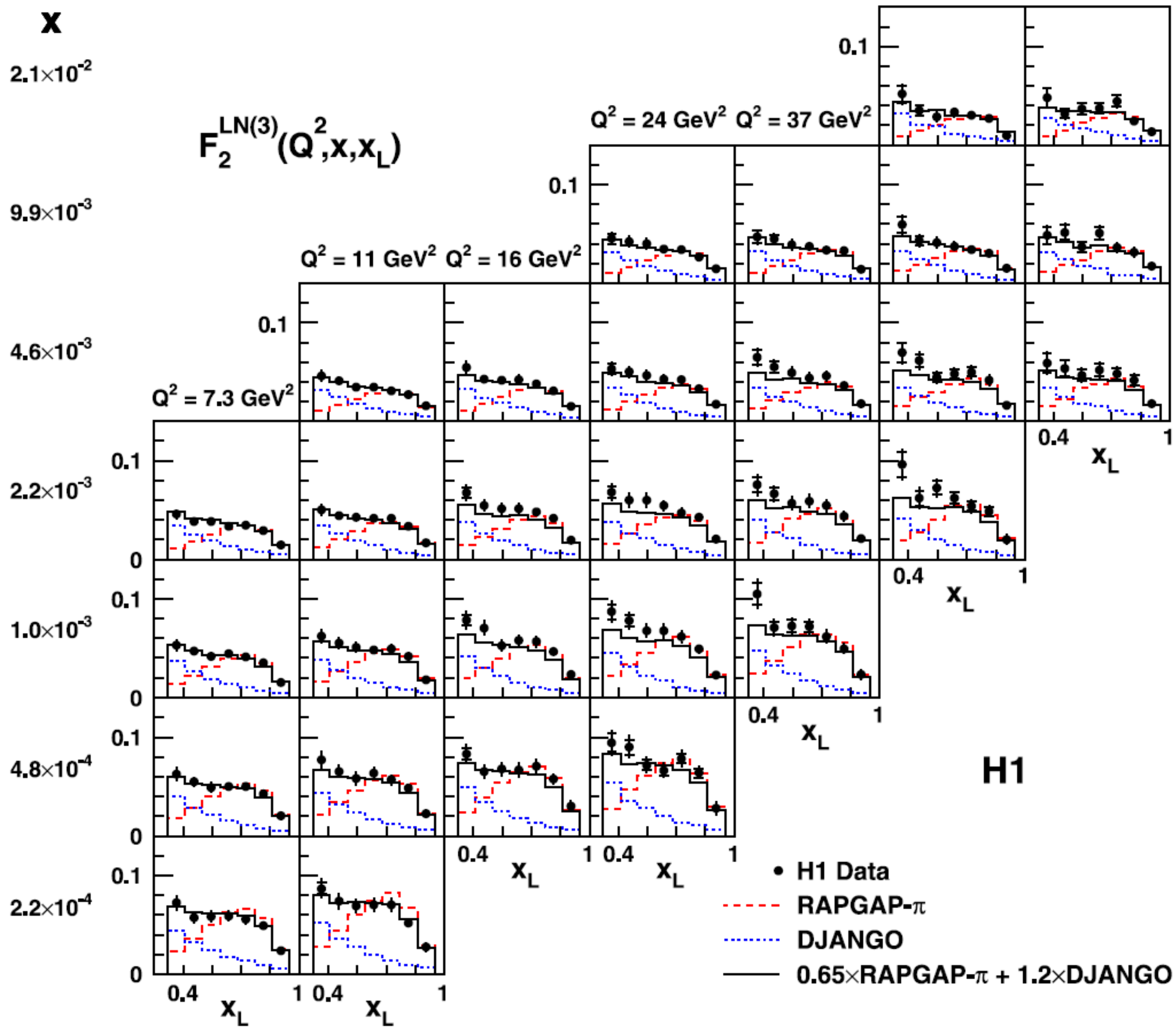
x
2.1×10-2
9.9×10-3
4.6×10-3
2.2×10-3
1.0×10-3
4.8×10-4
2.2×10-4
F2LN(3)(Q2,x,xL)
Q2 = 7.3 GeV2
Q2 = 11 GeV2
Q2 = 16 GeV2
Q2 = 24 GeV2
Q2 = 37 GeV2
0.1
0
0.4
1
xL
H1
H1 Data
RAPGAP-π
DJANGO
0.65×RAPGAP-π + 1.2×DJANGO

ZEUS

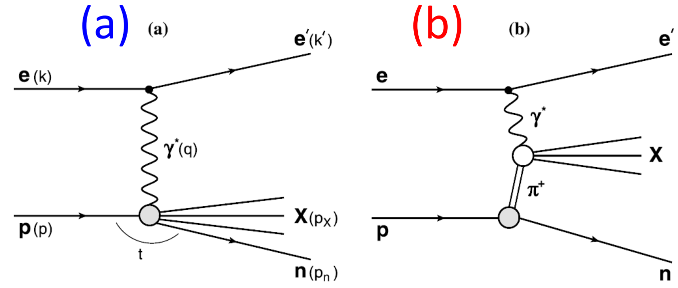

(a)
(a)
e (k)
e′(k′)
γ*(q)
p (p)
X(pX)
t
n (pn)
(b)
(b)
e
e′
γ*
X
π+
p
n

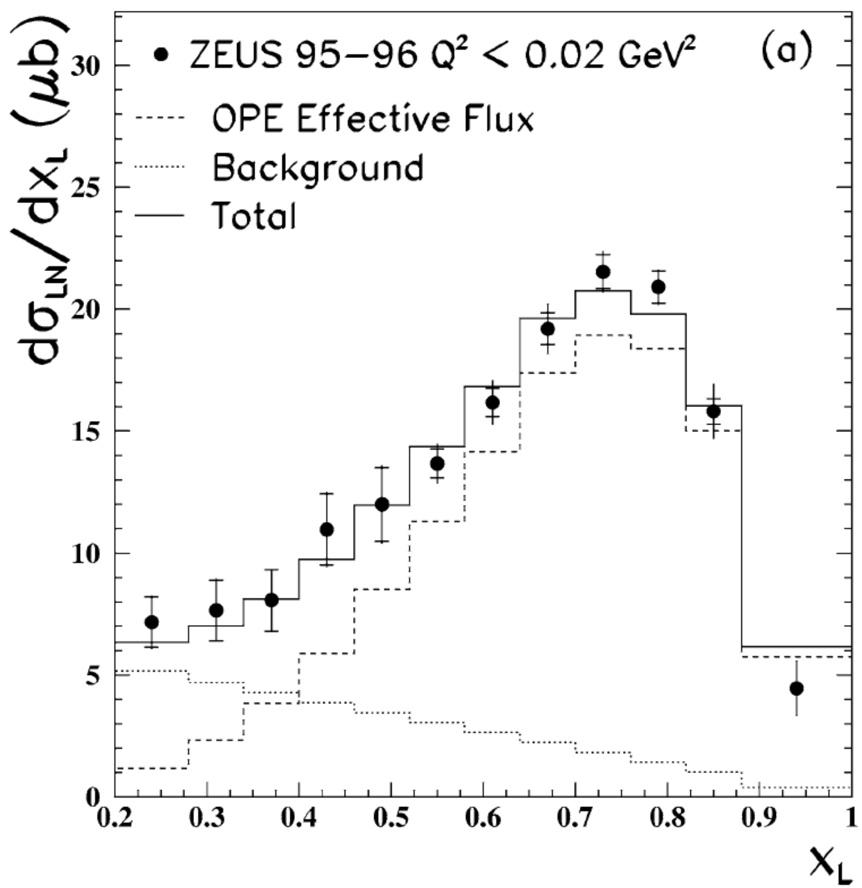

ZEUS 95–96 Q² < 0.02 GeV²
(a)
OPE Effective Flux
Background
Total
dσLN/dxL (μb)
30
25
20
15
10
5
0
0.2
0.3
0.4
0.5
0.6
0.7
0.8
0.9
1
xL

ZEUS

$$r(x, Q^2, x_L) = \frac{d^3\sigma^{ep\to e'Xn}/dx\,dQ^2\,dx_L}{d^2\sigma^{ep\to e'X}/dx\,dQ^2}\Delta x_L = \frac{n_{obs}(x, Q^2, x_L)}{A(x_L)N_{obs}(x, Q^2)},$$

$$F_2^{LN(3)}(x, Q^2, x_L) = \frac{r(x, Q^2, x_L)}{\Delta x_L} F_2(x, Q^2)$$

$$F_2^{LN(3)}(x, Q^2, x_L) = 2f_{\pi N}(\bar{x}_L)F_2^{\pi}(x_\pi, Q^2).$$

$$F_2^{\pi}(x_\pi) = \frac{r(x, x_L)}{\Delta x_L} F_2^P(x) \frac{1}{2f_{\pi N}(\bar{x}_L)}$$

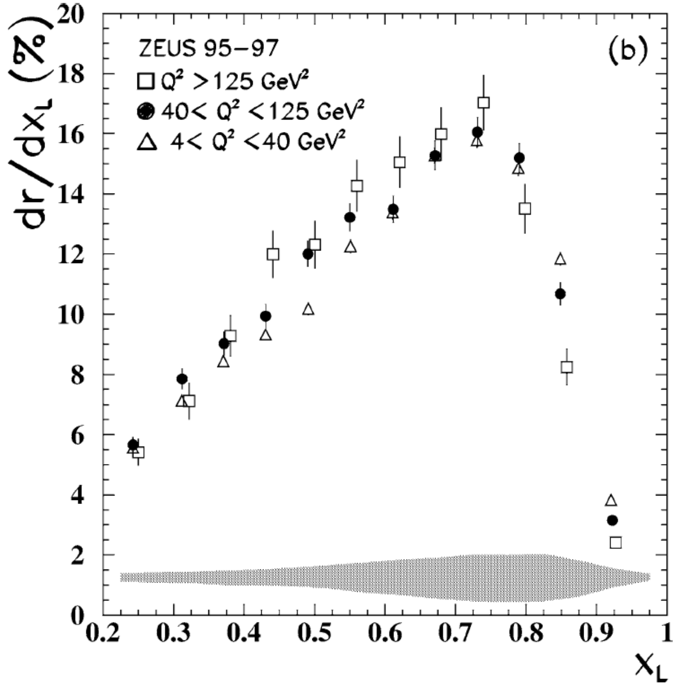

ZEUS

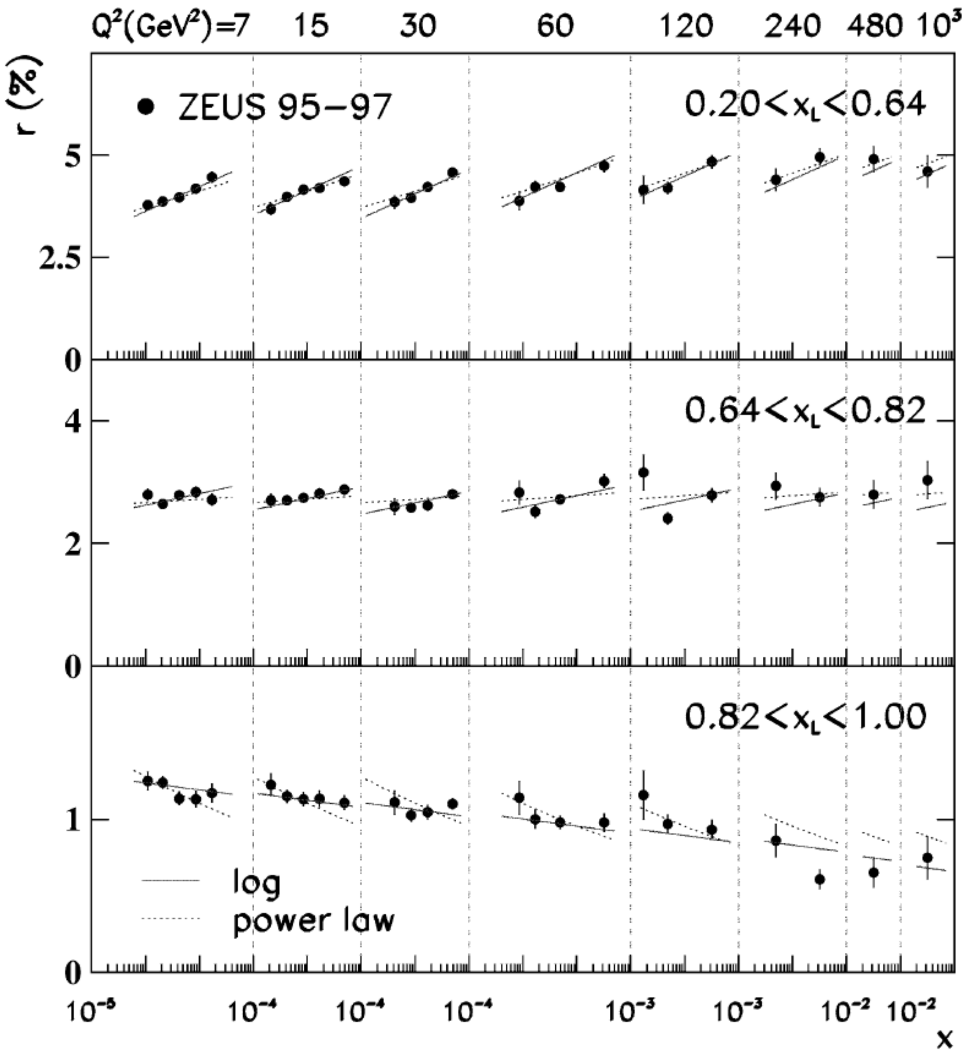

Q²(GeV²)=7
15
30
60
120
240
480
10³
r (%)
ZEUS 95−97
0.20<x_L<0.64
0.64<x_L<0.82
0.82<x_L<1.00
log
power law
10⁻⁵
10⁻⁴
10⁻⁴
10⁻⁴
10⁻³
10⁻³
10⁻²
10⁻²
x

H1

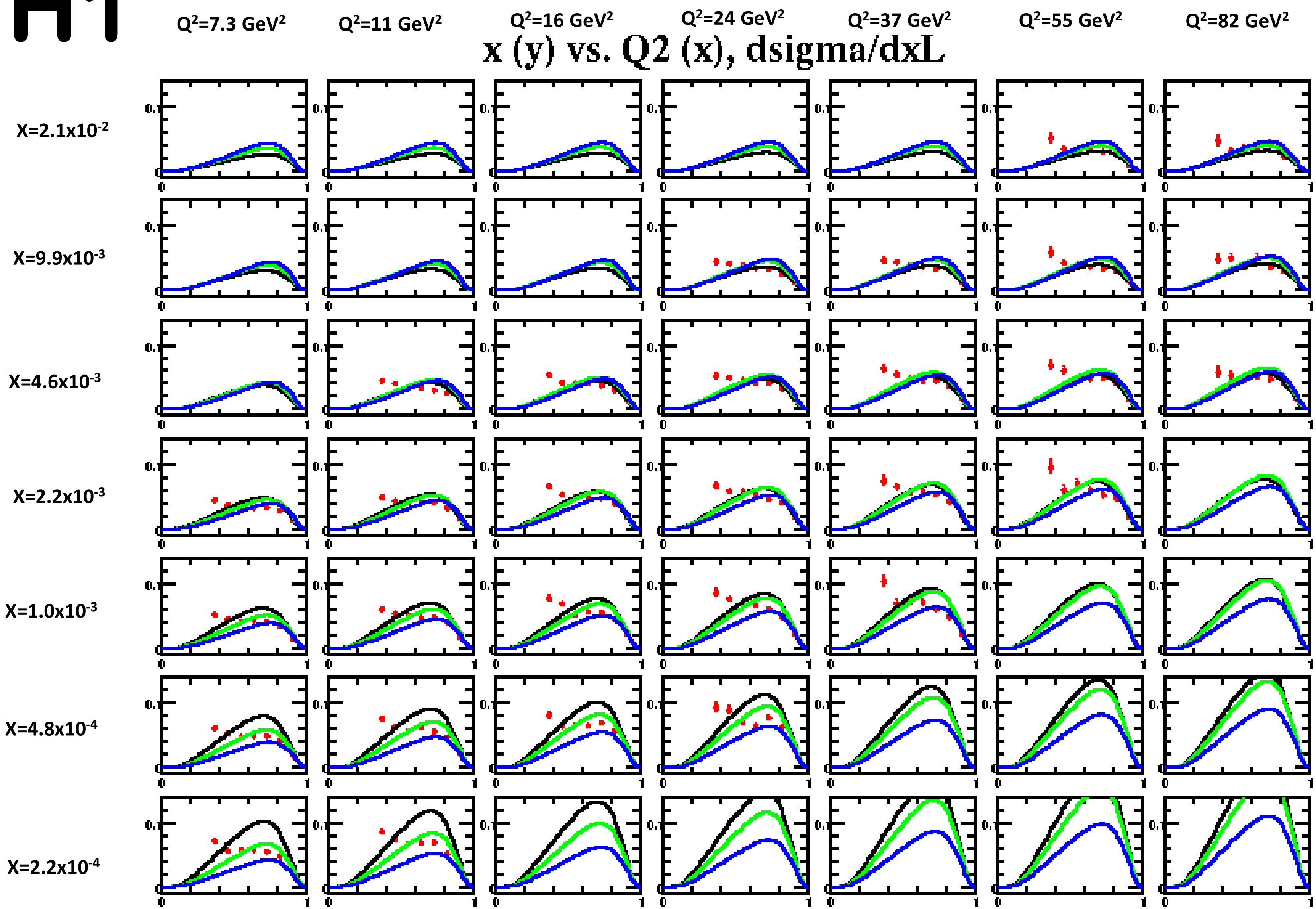

GRV, JAM, xFitter

$$x_L = \frac{E_n}{E_p}$$

ZEUS: Q2=60 GeV2

GRV, JAM, xFitter

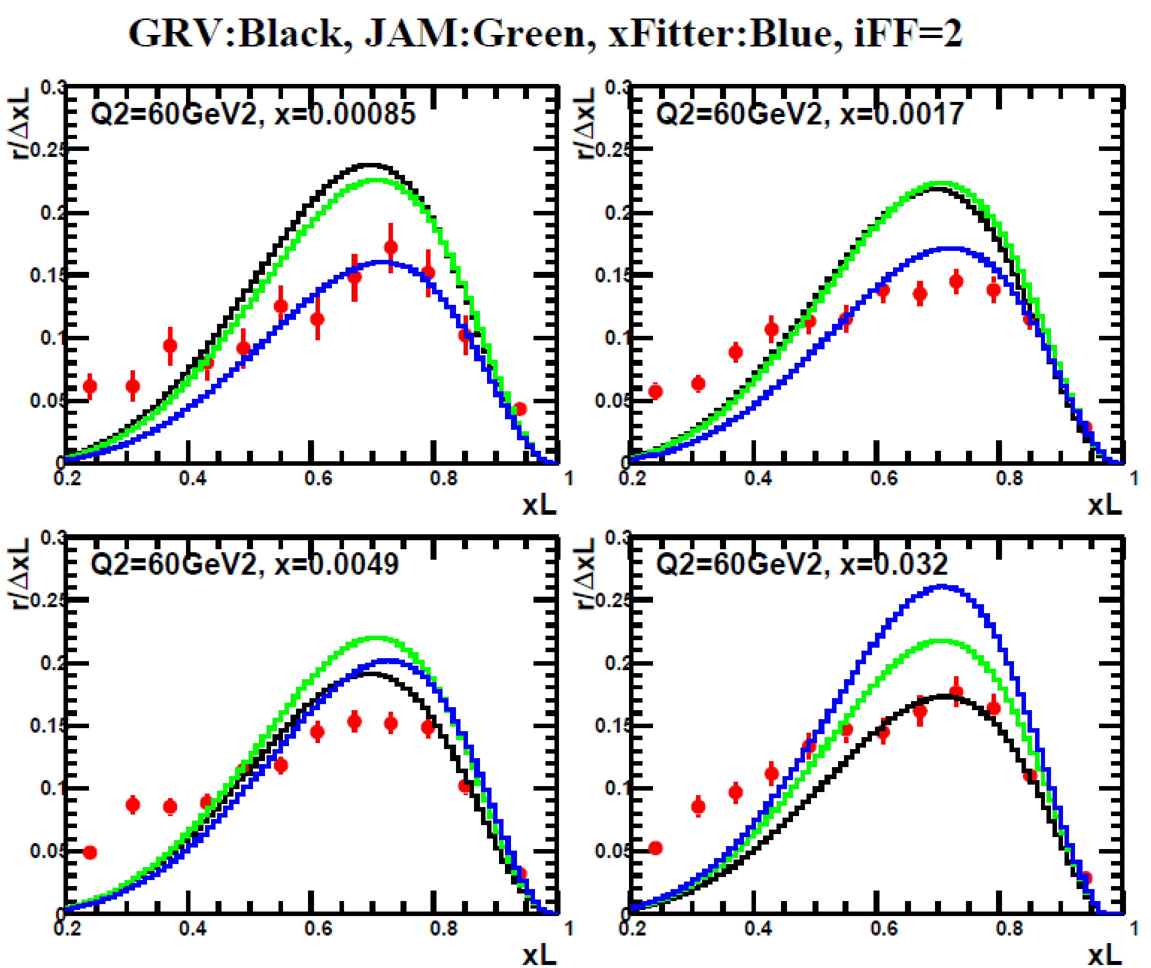

Ultraperipheral collisions (UPCs) Heavy quark photoproduction by photon - pion interactions

https://arxiv.org/abs/2512.13257

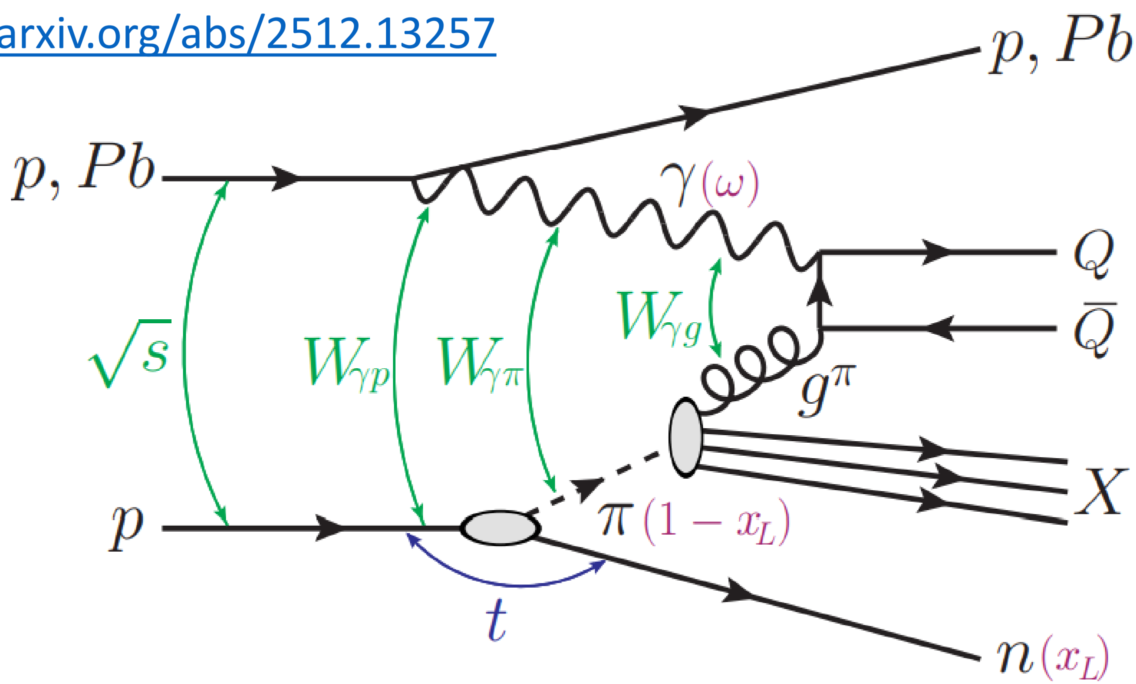

The final state will be characterized by the presence of a rapidity gap and a leading neutron, which can be tagged using a Zero Degree Calorimeter (ZDC).

QQ photoproduction

$$\frac{d\sigma\left[h_1+h_2\to h_i+Q\bar{Q}+X+n\right]}{dY} = \left[\omega\frac{dN}{d\omega}\bigg|_{h_1}\sigma_{\gamma h_2\to Q\bar{Q}+X+n}\left(\omega\right)\right]_{\omega_L} + \left[\omega\frac{dN}{d\omega}\bigg|_{h_2}\sigma_{\gamma h_1\to Q\bar{Q}+X+n}\left(\omega\right)\right]_{\omega_R}$$

Photon flux

Sullivan Process: $\gamma\pi$ Interations

In order to describe the cross-section $\sigma_{\gamma h \to Q\bar{Q}+X+n}$ we will assume the Sullivan process [32], which implies that it can be expressed as follows (See e.g. Ref. [40])

$$\sigma_{\gamma p \to Q\bar{Q}+X+n}(W^2_{\gamma p}) = \mathcal{K} \cdot \int dx_L dt \, f_{\pi/p}(x_L, t) \cdot \sigma_{\gamma\pi \to Q\bar{Q}+X}(W^2_{\gamma\pi}) \,, \qquad (6)$$

where $\mathcal{K}$ represents the absorption factor associated to soft rescatterings between the produced and spectator particles[1] and $f_{\pi/p}(x_L, t)$ is the pion flux. The main assumption here is that the splitting $p \to \pi^+ n$, the photon – pion interaction and the absorptive effects can be factorized. The general form of the pion flux is given by

$$f_{\pi/p}(x_L, t) = \frac{1}{4\pi} \frac{2g^2_{p\pi p}}{4\pi} \frac{-t}{(t - m^2_\pi)^2} (1 - x_L)^{1-2\alpha(t)} [F(x_L, t)]^2 \qquad (7)$$

where $g^2_{p\pi p}/(4\pi) = 14.5$ is the $p\pi p$ coupling constant, m_π is the pion mass, $\alpha(t)$ is the pion intercept and the form factor $F(x_L, t)$ accounts for the finite size of the nucleon and pion. Following Refs. [40, 41], we will assume an exponential form factor given by

$$F(x_L, t) = \exp[b(t - m^2_\pi)] \quad , \quad \alpha(t) = t \qquad (8)$$

https://arxiv.org/abs/2512.13257

QQ Photoproduction from π

to constrain $f_{\pi/p}$, reducing the dependence of our predictions on this assumption. Finally, in this exploratory study, the heavy quark photoproduction in photon-pion interactions will be estimated at leading order, which implies that the associated cross-section will be given by [42]

QQ photoproduction from pion

$$\sigma^{\gamma\pi\to Q\bar{Q}X}(W_{\gamma\pi}^2) = \int_{x_{min}}^{1} dx\ \sigma^{\gamma g\to Q\bar{Q}}(W_{\gamma g}^2)\, g^{\pi}(x,\mu^2), \qquad (9)$$

Gluon in pion

with $x_{min} = 4m_Q^2/W_{\gamma\pi}^2$ and

$$\sigma^{\gamma g\to Q\bar{Q}}(W_{\gamma g}^2) = \frac{2\pi\alpha_{em}\alpha_s(\mu^2)e_Q^2}{W_{\gamma g}^2}\left[\left(1+\beta-\frac{\beta^2}{2}\right)\ln\left(\frac{1+\nu}{1-\nu}\right)-(1+\beta)\nu\right], \qquad (10)$$

where $\nu = \sqrt{1-\beta}$ and $\beta = 4m_Q^2/W_{\gamma g}^2$. In our calculations, we will assume $\mu = 2\,m_Q$, with $m_c = 1.5$ GeV and $m_b = 4.5$ GeV, and $\mathcal{K} = 0.8$, which allow us to describe the HERA data for the leading neutron electroproduction [40].

https://arxiv.org/abs/2512.13257

Gluon in Pion PDFs

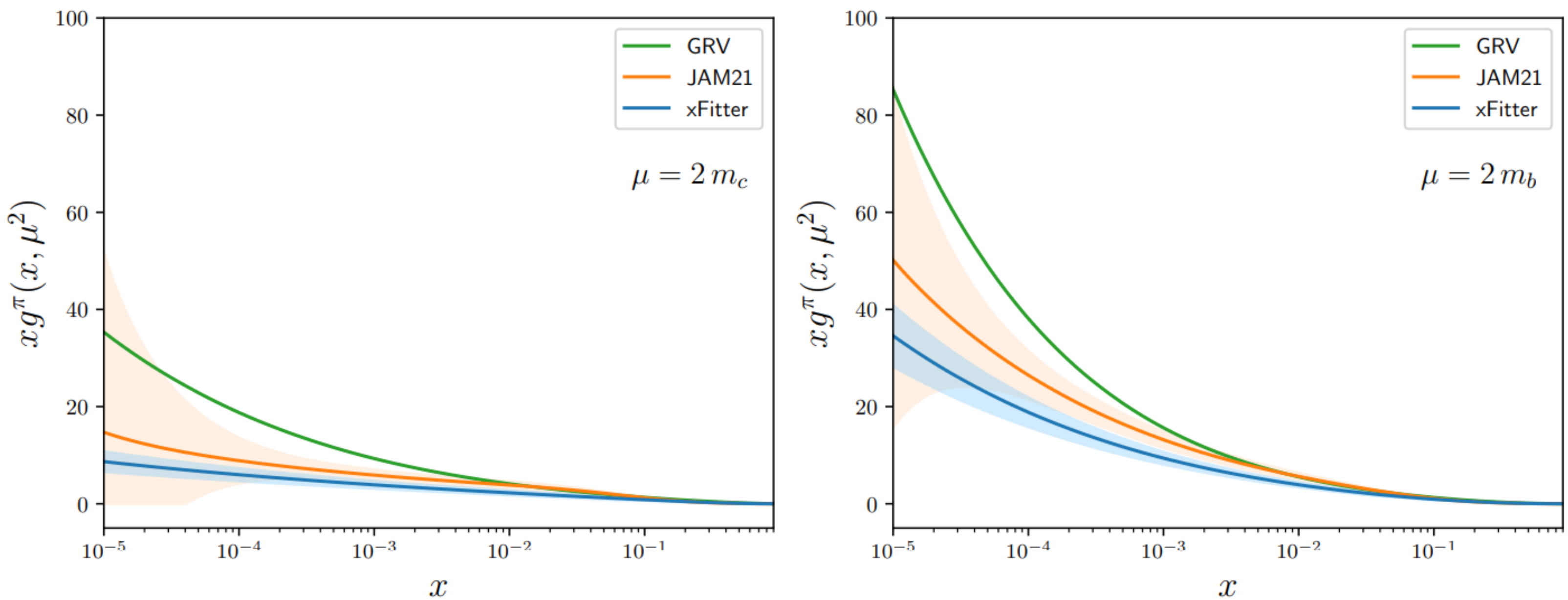

https://arxiv.org/abs/2512.13257

QQ photoproduction from pion

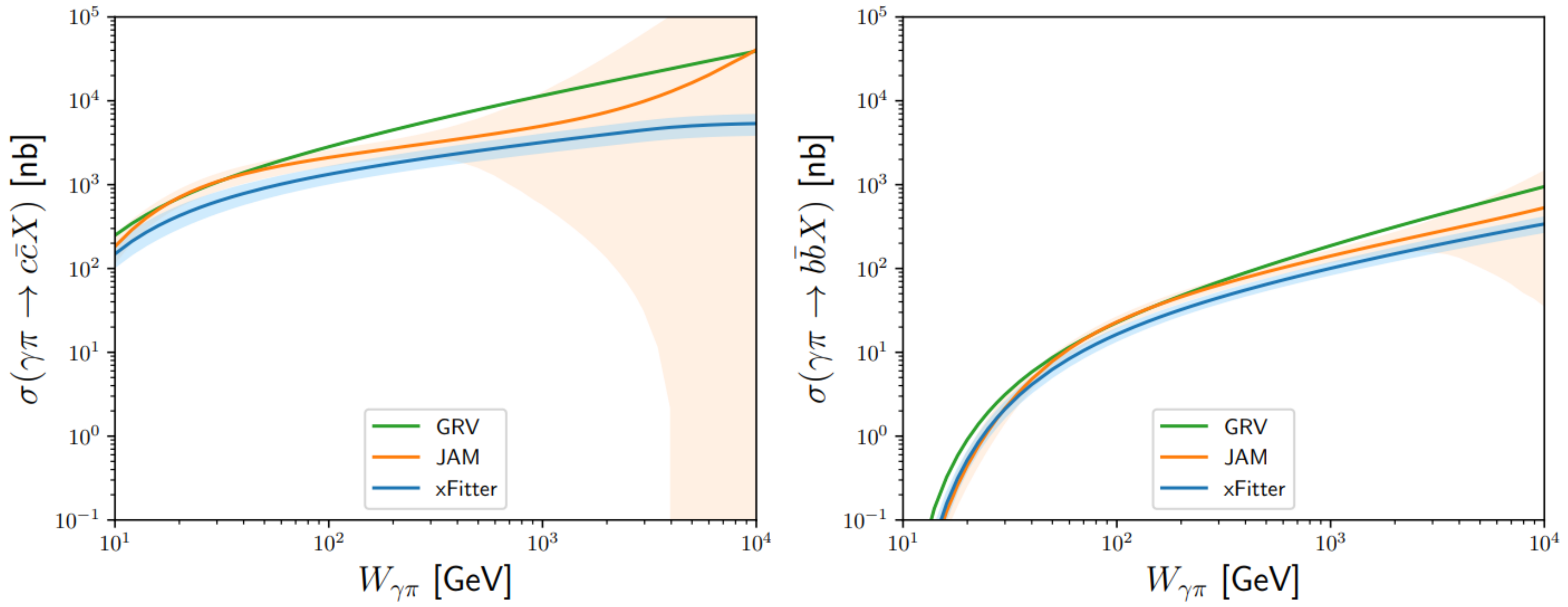

https://arxiv.org/abs/2512.13257

Rapidity distributions for the charm and bottom pair photoproduction

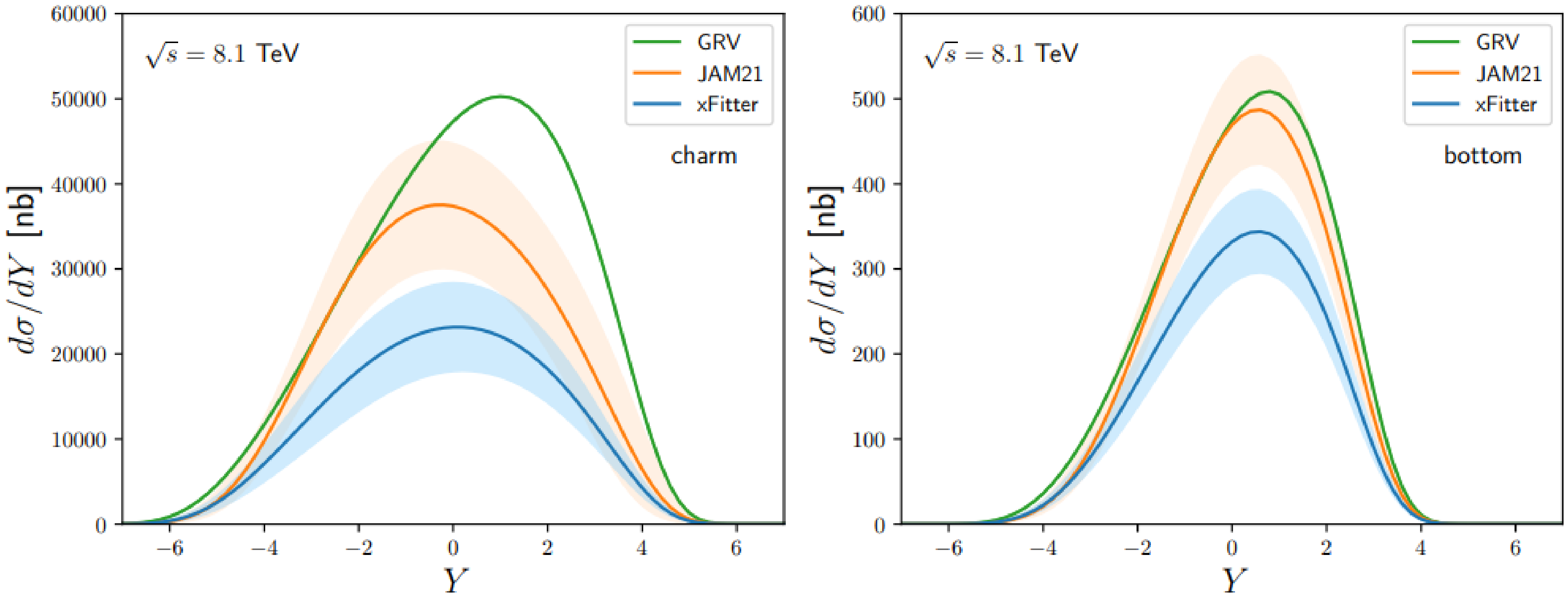

https://arxiv.org/abs/2512.13257

Rapidity distributions for the charm and bottom pair photoproduction

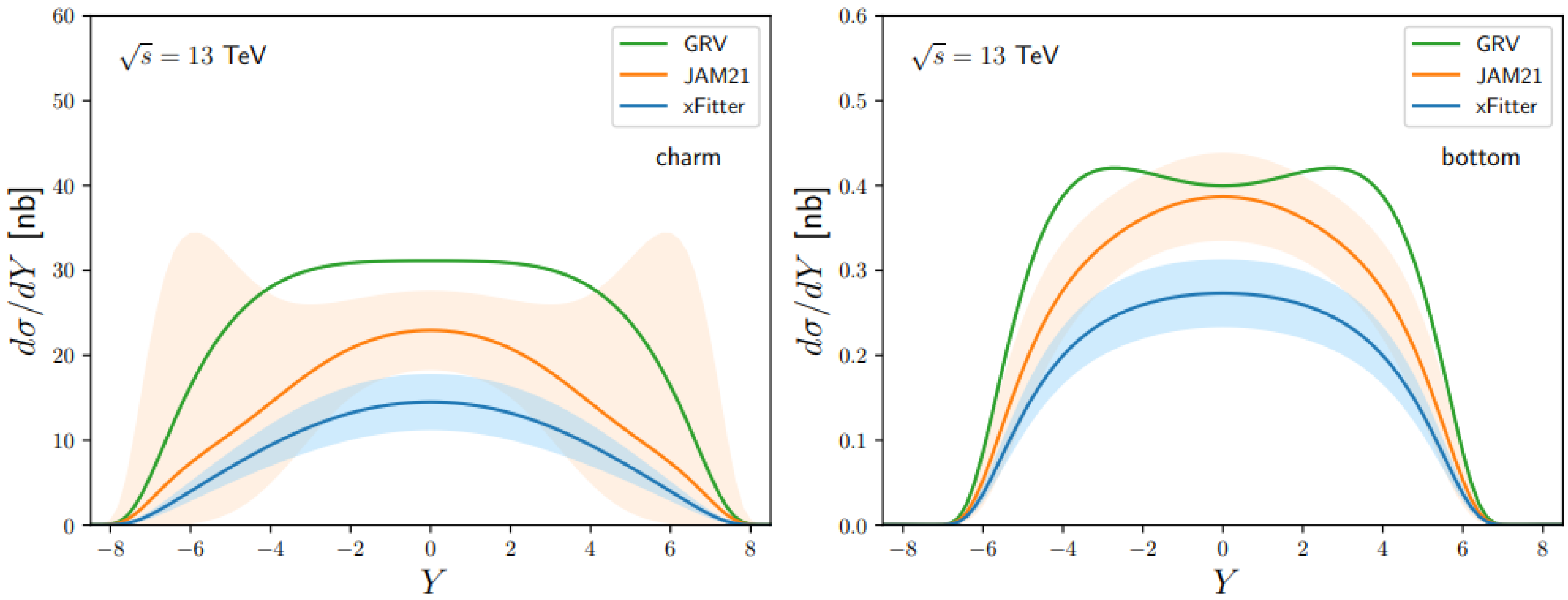

https://arxiv.org/abs/2512.13257

Theoretical Formulation PRD 93, 054011 (2016)

PHYSICAL REVIEW D **93,** 054011 (2016)

Pion structure function from leading neutron electroproduction and SU(2) flavor asymmetry

J. R. McKenney,[1,2,3] Nobuo Sato,[2] W. Melnitchouk,[2] and Chueng-Ryong Ji[1]

[1] *North Carolina State University, Raleigh, North Carolina 27695, USA*
[2] *Jefferson Lab, Newport News, Virginia 23606, USA*
[3] *University of North Carolina, Chapel Hill, North Carolina 27599, USA*

(Received 15 December 2015; published 7 March 2016)

We examine the efficacy of pion exchange models to simultaneously describe leading neutron electroproduction at HERA and the $\bar{d} - \bar{u}$ flavor asymmetry in the proton. A detailed χ^2 analysis of the ZEUS and H1 cross sections, when combined with constraints on the pion flux from Drell-Yan data, allows regions of applicability of one-pion exchange to be delineated. The analysis disfavors several models of the pion flux used in the literature and yields an improved extraction of the pion structure function and its uncertainties at parton momentum fractions in the pion of $4 \times 10^{-4} \lesssim x_\pi \lesssim 0.05$ at a scale of $Q^2 = 10$ GeV^2. Based on the fit results, we provide estimates for leading proton structure functions in upcoming tagged deep-inelastic scattering experiments at Jefferson Lab on the deuteron with forward protons.

DOI: 10.1103/PhysRevD.93.054011

MC Simulations

https://eic.github.io/software/mcgen.html

Monte Carlo simulations are used to correct the data for the effects of detector acceptance, inefficiencies and migrations between measurement intervals due to finite resolution and QED radiation. All generated events are passed through a GEANT3 [33] based simulation of the H1 apparatus and are processed using the same reconstruction and analysis framework as is used for the data.

The DJANGO [34] program generates inclusive DIS events. It is based on leading order electroweak cross sections and takes QCD effects into account up to order α_s. The hadronic final state is simulated using ARIADNE [35], based on the Colour Dipole Model, with subsequent hadronisation effects modelled using the Lund string fragmentation model as implemented in JETSET [36]. DJANGO is also used in this analysis to simulate events where leading neutrons originate from proton remnant fragmentation. RAPGAP [37] is a general purpose event generator for inclusive and diffractive ep interactions. Higher order QCD effects are simulated using parton showers and the final state hadrons are obtained via Lund string fragmentation. Higher order electroweak processes in the DJANGO and RAPGAP generators are simulated using an interface to HERACLES [38].

Monte Carlo Event Generators

- PYTHIA6
- BeAGLE
- DJANGOH
- MILOU
- RAPGAP
- PEPSI
- elSpectro
- EpIC (Pawel Sznajder)
- TOPEG (Orsay Perugia)
- eSTARlight
- Sartre

DJANGOH

https://github.com/spiesber/DJANGOH

README

DJANGOH - version 4.6.21 (05.05.2022)

Monte Carlo simulation for deep inelastic lepton nucleon scattering

DJANGOH performs event simulation of neutral and charged current lepton nucleon scattering. The program was developed originally for deep inelastic electron proton scattering at HERA, but has been extended and includes options for muon scattering, heavy nuclear targets, elastic scattering and polarized protons. The emphasis is put on the inclusion of radiative corrections, comprising single soft and hard photon emission and the complete set of electroweak 1-loop corrections in the Standard Model. Large-mass hadronic final states are generated by an interface to LEPTO which simulates QCD effects. Low-mass hadronic final states are included by an interface to SOPHIA.

Please send complaints, observations, suggestions to spiesber@uni-mainz.de

RAPGAP

https://rapgap.hepforge.org/
https://gitlab.cern.ch/jung/rapgap

RAPGAP
Hadron level Monte Carlo generator for ep and selected processes in pp scattering

The Monte Carlo program RAPGAP generates a full hadron event record according to the HEP common standards. In ep it can describe all inclusive and diffractive processes, in pp it is available for single-diffractive and a few inclusive processes for heavy quark and jet production.

posted 2021-12-19
Version 3.308 of RAPGAP has now been released.
This release includes autotools installation features, as well as optionally wrting output in HepMC format for further use with Rivet. No need to link PYTHIA6 and ARIADNE externally, source code is included in distribution. Updates writing hepmc files are included by A. Verbytskyi.

The source code is now also availbale from gitlab and from download

The full manual is also distributed in the download

Older versions can be found on here

To receive announcements of new releases for RAPGAP, send an email to Hannes Jung

Credits and Blame

Many people have contributed to the functionality and stability of RAPGAP, especially from the HERA experiment H1 and ZEUS, where the program is extensively used.

Summary

- Sullivan process is an interesting experimental approach where the meson PDFs could be explored in the UPCs at LHC and the DIS at EIC.
- The ZDC is a key component of tagging this process.
- The exercising of DJANGOH and RAPGAP event generators will be helpful for understanding the background, optimization of ZDCs design and feasibility study of physics measurements in EIC.